COMPUTING DECOUPLED RESIDUALS FOR COMPACT DISC PLAYERS

Peter Fogh Odgaard * **Jakob Stoustrup** *
Enrique Vidal **

* *Department of Control Engineering, Aalborg University, Aalborg, Denmark, odgaard@control.aau.dk*
** *Bang & Olufsen a/s, Peter Bangs Vej 15, DK-7600 Struer, Denmark, evs@bang-olufsen.dk*

Abstract
In order to improve Compact Disc Players playability regarding playing Compact Discs with surface faults, like scratches and fingerprints etc, the attention has been put on fault tolerant control schemes. Almost every of those methods are based on fault detection. The standard approach is to use a pair of residuals generated by Compact Disc Player. However, these residuals depend on the performance of position servos in the Compact Disc Player. In other publications of the same authors a pair of decoupled residuals is derived. However, the computation of these alternative residuals has been based on iterative methods. In this paper an algebraic solution is presented. The algebraic algorithm do only use two thirds of the number of multiplication and additions as the iterative method uses per iteration.

Keywords: Fault Detection, CD Rom, Control Applications, Residues, Detection algorithms

1. INTRODUCTION

Optical disc players have in the last couple of decades been one of the preferred storage medias. In the following a specific optical disc player will be dealt with, it is the Compact Disc Players (CD-Players). However, surface faults on the disc, like scratches and fingerprints, can cause problems retrieving the stored information from this faulty disc. One reason for this problem is to be found in the control loops positioning the Optical Pick-up Unit (OPU). The OPU is used to retrieve the information stored on the disc in a spiral shaped track. The OPU works by emitting a laser beam, and by following detecting the part of the laser beam reflected by the disc. In order to receive the correct reflections the OPU is positioned in two directions. The laser beam is focused on the track, meaning that the focus displacement e_{f} is minimized, and it is radially positioned at the track, meaning that the radial displacement e_{r} is minimized. These two displacements are illustrated in Fig. 1. Two control servos are formed to minimize these two displacements as much as possible. A linear electro-magnetic actuator is used to position the OPU in each of the two directions. The OPU also generates four detector signals, (two focus detectors and two radial detectors), which depend on focus and radial displacements. The CD-Player is described more detailed in (Bouwhuis *et al.* 1985).

A large number of different control strategies have been applied in the design of these controllers, some examples of different applied control strategies are mentioned in the following. (Steinbuch *et*

al. 1992) was the first example of a μ-controller design to a CD-Player based on DK-iterations. An example of an adaptive control design was (Draijer *et al.* 1992) where a self-tuning controller was suggested. In the following years a large number of different control strategies has been applied to the CD-Players.

These designs are designed with the purpose of controlling Players playing CDs without surface faults like scratches and fingerprints. The problem with these surface faults is that during a fault the displacement sensor information from the OPU contains an additional faulty component due to the surface faults. The sensor signals are used by the servo controllers to position the OPU in the focus and radial directions. This means that if nothing is done in order to accommodate the faults, the controllers will react on these fault components and in the worst case force the OPU out of tracking and/or focus.

The design of controllers which accommodates the surface faults on the discs, have been more limited, see (Philips 1994), (Andersen *et al.* 2001), (Vidal Sánchez 2003) and (Odgaard 2004). All these accommodation schemes are based on a detection of the faults. The standard residual used for the detection can easily be computed based on the four detector signals from the OPU. A focus residual can be computed by adding the two focus detector signals, and a radial residual can be computed by adding the two radial detector signals, (Bierhoff 1984). However, the focus residual depends on the radial position of the OPU and the radial residual depends on the focus position of the OPU. This can result in a lowering of the performance of the fault detection. In (Odgaard *et al.* 2006) and (Odgaard 2004) a pair of decoupled residuals are suggested, these residuals are given by a model of the surface faults.

These decoupled residuals, as well as the displacements are not directly measurable. The relation from these signals to the detector signals can be represented by a non-linear multi-variable static mapping. This means that the inverse of this mapping is required in order compute residuals and displacements. However, this mapping is not globally invertible. The mappings can be approximated by second order separable splines, see (Odgaard *et al.* 2006). Since the approximating splines consist of second order polynomials it is possible to derive an algebraic inverse map, if the region of displacements and residuals are known. Due to the mechanics of the CD-Player the change in displacements and residuals is limited so much that previous displacements and residuals can be used to chose these polynomials. If the previous point was near the edge of defined interval of the given polynomial, it might end up in the defined interval of the neighbor polynomials. This means it is possible to compute the alternative decoupled residuals by an algebraic method, instead of using the iterative solution described in (Odgaard *et al.* 2006) and (Odgaard 2004).

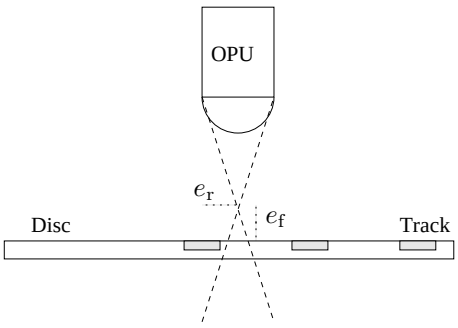

Figure 1. The focus displacement, e_f, is the displacement from the focus point of the laser beam to the reflection layer of the disc, the radial displacement, e_r, is the displacement from the center of the laser beam to the center of the track.

This paper presents an algebraic solution to the inverse mapping of the combined optical and fault model in CD-Players. The combined optical and fault model is presented, which makes it possible to derive the algebraic inverse of this model. The algebraic inverse is subsequently tested with simulations. An example of the improvement by using the computed residual is showed by comparison with the normally used threshold. Finally the paper is concluded.

2. THE COMBINED OPTICAL AND FAULT MODEL

The used optical model is presented in (Odgaard *et al.* 2003). This model represents the relation from focus and radial distances to the four detector signals, in cases of no surface faults. The model is of the following structure

$$\left[D_1, D_2, S_1, S_2\right] = \mathbf{f}\left(e_f, e_r\right), \tag{1}$$

where D_1, D_2 are the two focus detector signals, S_1, S_2 are the two radial detector signals, and $\mathbf{f}(\cdot)$ is a vector function representing the optical mapping (model). In (Odgaard *et al.* 2003) this model is approximated by

$$\left[D_1, D_2, S_1, S_2\right] = \mathbf{h}\left(e_f\right) \cdot \mathbf{g}\left(e_r\right). \tag{2}$$

Each of the functions in (2) can be approximated by second order splines. By using spline approximations of the mappings the optical model can be given by

$$D_1 = h_1(e_f) \cdot g_1(e_r), \tag{3}$$
$$D_2 = h_2(e_f) \cdot g_2(e_r), \tag{4}$$
$$S_1 = h_3(e_f) \cdot g_3(e_r), \tag{5}$$
$$S_2 = h_4(e_f) \cdot g_4(e_r), \tag{6}$$

where h_i and g_i are the polynomial splines approximating the functions in the optical model, ($i \in \{1,2,3,4\}$). Two of these functions represent the physical variable, these are $g_1(e_\mathrm{r})$ and $g_2(e_\mathrm{r})$, see (Odgaard *et al.* 2003). This means that the optical model can be simplified by

$$g_1(e_\mathrm{r}) = g_2(e_\mathrm{r}) \tag{7}$$

All the functions can partly be approximated with second or first order polynomials, and those forms the splines.

2.1 Fault model

In (Odgaard *et al.* 2006) and (Odgaard 2004) the surface faults are modeled as scalings of the output of the optical model. The surface faults can be modeled as scalings of the detector signals, since a surface fault results in less received light energy at the photo detectors. The fracture in the disc surface will result in light being reflected in other directions than the intended one.

It is the objective of the combined optical and fault model to represent both responses of the detector signals to displacements and surface faults. This model is required to have an output in $\mathcal{R}^4$ (the four detector signals). Due to requirements of invertiability the inputs is also in $\mathcal{R}^4$. Two of the input signals are given as the two displacement positions e_f and e_r. This means that the fault can be represented by only two parameters. In (Odgaard *et al.* 2006) and (Odgaard 2004) these parameters have been defined as being a scaling of the two focus detector signals, β_f, and a scaling of the two radial detector signals, β_r. A residual is in (Chen and Patton 1999) defined as being zero in case of no fault and one in case of a fault. In (Odgaard 2004) these scalings, which models the surface faults, where transformed into two residuals. The focus residual is defined as $\alpha_\mathrm{f} = 1 - \beta_\mathrm{f}$, and the radial residual is defined as $\alpha_\mathrm{r} = 1 - \beta_\mathrm{r}$. Combining these scalings with the approximated optical model, given in (3-6), result in the following combined model

$$D_1 = (1-\alpha_\mathrm{f}) \cdot h_1(e_\mathrm{f}) \cdot g_1(e_\mathrm{r}), \tag{8}$$
$$D_2 = (1-\alpha_\mathrm{f}) \cdot h_2(e_\mathrm{f}) \cdot g_2(e_\mathrm{r}), \tag{9}$$
$$S_1 = (1-\alpha_\mathrm{r}) \cdot h_3(e_\mathrm{f}) \cdot g_3(e_\mathrm{r}), \tag{10}$$
$$S_2 = (1-\alpha_\mathrm{r}) \cdot h_4(e_\mathrm{f}) \cdot g_4(e_\mathrm{r}). \tag{11}$$

The subsequent objective is to find a method for computing the inverse of this mapping given that e_f and e_r are in a known region, (in order to chose the correct second order polynomial splines).

3. COMPUTATION OF THE INVERSE MAP

In this section an algebraic inverse map of the combined optical and fault model is derived. It is assumed that the region of the two displacements are known, these will be known if computation of the inverses starts while the OPU is the normal operational range in both directions. I.e. the correct polynomials can be chosen for the approximation. The previously computed displacements are used to choose the initial approximating polynomial, since maximum displacement change from sample to sample is limited.

The first step is to compute e_f. If (8-9) are combined with (7), equation (12) can be stated

$$\frac{D_1}{h_1(e_\mathrm{f})} = \frac{D_2}{h_2(e_\mathrm{f})} \Rightarrow \tag{12}$$
$$D_1 \cdot h_2(e_\mathrm{f}) - D_2 \cdot h_1(e_\mathrm{f}) = 0, \tag{13}$$

$h_1(e_\mathrm{f})$ and $h_2(e_\mathrm{f})$ can be approximated by second order polynomial splines for the given intervals. I.e. $h_1(e_\mathrm{f}) = h_{1,2} \cdot e_\mathrm{f}^2 + h_{1,1} \cdot e_\mathrm{f} + h_{1,0}$, and $h_2(e_\mathrm{f}) = h_{2,2} \cdot e_\mathrm{f}^2 + h_{2,1} \cdot e_\mathrm{f} + h_{2,0}$. The solution to (13) is subsequently given by

$$e_\mathrm{f} = \frac{-(h'_{2,1} - h'_{1,1}) + \sqrt{Q}}{2 \cdot \left(h'_{2,2} - h'_{1,2}\right)}, \tag{14}$$

where

$$Q = (h'_{2,1} - h'_{1,1})^2 - 4 \cdot (h'_{2,2} - h'_{1,2}) \cdot (h'_{2,0} - h'_{1,0}), \tag{15}$$
$$h'_1 = D_2 \cdot h_1 \ \wedge \ h'_2 = D_1 \cdot h_2. \tag{16}$$

This solution is only valid if $h'_{2,2} \neq h'_{1,2} \vee Q \geq 0$. This requirement is fulfilled by the practical setup, and the resulting used polynomial splines. Only the given solution of the second order equation is possible, since the other solution is outside the defined interval for the given approximating polynomials.

The second step is to compute e_r based on (10-11) and the computed value of e_f. The following equation can be stated.

$$\frac{S_1}{h_3(e_\mathrm{f}) \cdot g_3(e_\mathrm{r})} = \frac{S_2}{h_4(e_\mathrm{f}) \cdot g_4(e_\mathrm{r})} \Rightarrow \tag{17}$$
$$S_1 \cdot h_4(e_\mathrm{f}) \cdot g_4(e_\mathrm{r}) - S_2 \cdot h_3(e_\mathrm{f}) \cdot g_3(e_\mathrm{r}) = 0. \tag{18}$$

Second order polynomials are used for the approximations meaning,

$$e_\mathrm{r} = \frac{-(g'_{4,1} - g'_{3,1}) + \sqrt{Q}}{2 \cdot (g'_{4,2} - g'_{3,2})}, \tag{19}$$

where

$$Q = (g'_{4,1} - g'_{3,1})^2 - 4 \cdot (g'_{4,2} - g'_{3,2}) \cdot (g'_{4,0} - g'_{3,0}), \tag{20}$$
$$g'_3 = h_3(e_\mathrm{f}) \cdot S_2 \cdot g_3 \ \wedge \ g'_2 = h_4(e_\mathrm{f}) \cdot S_1 \cdot g_2. \tag{21}$$

The solution in (19) is only valid if $g'_{4,2} \neq g'_{3,2} \vee Q \geq 0$. This requirement is fulfilled by the practical setup, and the resulting used polynomials. Only the positive solution of the second order equation is inside the defined interval of the given

approximating polynomial. In situations where the wrong polynomials are chosen, the positive solution is closest to the correct solution. This can subsequently be used to chose the correct approximating polynomial.

The two residuals α_{f} and α_{r} are subsequently computed. After computing focus and radial displacements, one ends up with four equations with two variables, where two of the equations only have one variable and the other two equations depend on the second variable.

$$\begin{bmatrix} h_1(e_{\mathrm{f}}) \cdot g_1(e_{\mathrm{r}}) \\ h_2(e_{\mathrm{f}}) \cdot g_1(e_{\mathrm{r}}) \end{bmatrix} \cdot \alpha_{\mathrm{f}} = \begin{bmatrix} D_1 \\ D_2 \end{bmatrix}, \tag{22}$$

$$\begin{bmatrix} h_3(e_{\mathrm{f}}) \cdot g_3(e_{\mathrm{r}}) \\ h_4(e_{\mathrm{f}}) \cdot g_4(e_{\mathrm{r}}) \end{bmatrix} \cdot \alpha_{\mathrm{r}} = \begin{bmatrix} S_1 \\ S_2 \end{bmatrix}. \tag{23}$$

The solutions can be given by taking the mean of each pair of equations. The mean is used since it in practice have given the best results. These can easily be computed by (24) and (25).

$$\alpha_{\mathrm{f}} = \frac{1}{2} \cdot \left(\frac{D_1}{h_1(e_{\mathrm{f}}) \cdot g_1(e_{\mathrm{r}})} + \frac{D_2}{h_2(e_{\mathrm{f}}) \cdot g_1(e_{\mathrm{r}})} \right), \tag{24}$$

$$\alpha_{\mathrm{r}} = \frac{1}{2} \cdot \left(\frac{S_1}{h_3(e_{\mathrm{f}}) \cdot g_3(e_{\mathrm{r}})} + \frac{S_2}{h_4(e_{\mathrm{f}}) \cdot g_4(e_{\mathrm{r}})} \right). \tag{25}$$

3.1 Handling change of approximating polynomial

It is clearly a problem if the computed displacements are outside the defined region of their related polynomials. However, this can be handled simply by changing the approximating polynomial to the ones indicated by the computed displacements. The displacements and residuals are following computed again by using the newly chosen approximating polynomials. The change of polynomials will only be relevant once, due to the limited displacement changes, since only a neighbor to the initial used polynomial can be relevant.

3.2 The algorithm

The algebraic method for computing $e_{\mathrm{f}}, e_{\mathrm{r}}, \alpha_{\mathrm{f}}, \alpha_{\mathrm{r}}$ is now found. The steps in the computation can be listed as:

(1) Compute: $e_{\mathrm{f}} = \frac{-(h'_{2,1}-h'_{1,1})+\sqrt{Q}}{2 \cdot h'_{2,2}-h'_{1,2}}$,
where
$Q = (h'_{2,1}-h'_{1,1})^2 - 4 \cdot (h'_{2,2}-h'_{1,2}) \cdot (h'_{2,0}-h'_{1,0})$,
$h'_1 = D_2 \cdot h_1 \ \wedge \ h'_2 = D_1 \cdot h_2$.

(2) Compute: $e_{\mathrm{r}} = \frac{-(g'_{4,1}-g'_{3,1})+\sqrt{Q}}{2 \cdot (g'_{4,2}-g'_{3,2})}$,
where
$Q = (g'_{4,1}-g'_{3,1})^2 - 4 \cdot (g'_{4,2}-g'_{3,2}) \cdot (g'_{4,0}-g'_{3,0})$,
$g'_3 = h_3(e_{\mathrm{f}}) \cdot S_2 \cdot g_3 \ \wedge \ g'_2 = h_4(e_{\mathrm{f}}) \cdot S_1 \cdot g_2$.

(3) If the computed values of e_{f} and e_{f} are inside the defined intervals of the used approximating polynomials proceed to step 4, if not change the approximating polynomials to the neighbor polynomials which defined interval contains the values of the computed displacements, and jump back to step 1.

(4) Compute: $\alpha_{\mathrm{f}} = \frac{1}{2} \cdot \left(\frac{D_1}{h_1(e_{\mathrm{f}}) \cdot g_1(e_{\mathrm{r}})} + \frac{D_2}{h_2(e_{\mathrm{f}}) \cdot g_1(e_{\mathrm{r}})} \right)$.

(5) Compute: $\alpha_{\mathrm{r}} = \frac{1}{2} \cdot \left(\frac{S_1}{h_3(e_{\mathrm{f}}) \cdot g_3(e_{\mathrm{r}})} + \frac{S_2}{h_4(e_{\mathrm{f}}) \cdot g_4(e_{\mathrm{r}})} \right)$.

3.3 Computational complexity

The main reason to use this implementation of the residual computation, instead of the iterative implementation, is to limit the number of required computations. All in all this algorithm requires approximately 45 multiplications and 20 additions. In the rear cases where the result is not in the definition set of the used polynomials these numbers are doubled. The iterative implementation, on the other hand, requires approximately 60 multiplications and 40 additions per iteration. Experiments with the iterative implementation have shown that normally 2 iterations are used and in rare case 3 iterations are used in order to achieve a low enough approximation error. This implies that the newly proposed implementation is faster in terms of computations than iterative algorithm.

4. SIMULATION OF AN EXAMPLE

In this section the algebraic method is tested by comparing its output with the original focus and radial displacements used for the simulation. The used input signals (e_{f} and e_{r}) to this simulation are two sine signals with a small difference in the frequency so that the two input signals are not fully correlated. The frequency and amplitude of these sine signals are chosen in a way that the maximum variance value from one sample to another is at least: 0.014μm, since it is the maximum position movement from sample to sample, see (Odgaard *et al.* 2006). The simulation is based on a simulation without any faults, see the upper figure in Fig. 2. This fault free signals is following multiplied with signals representing the surface fault in the four detector signals. The fault signal is constructed using the model in (8-11), where $1-\alpha$ represents the surface faults, and the used $1-\alpha$ signal is illustrated in the middle figure in Fig. 2. Using the fault model and the fault signal in middle figure in Fig. 2, the simulation series of samples with surface faults are computed and illustrated in the lower figure in Fig. 2.

The algebraic solution algorithm is subsequently applied to the signals illustrated in the lower figure in Fig. 2. In Fig. 3, the computed focus and radial displacements are compared with the original ones. From the upper plot in Fig. 3 it can be seen that the algebraic solution ends up with small computation errors. These errors are

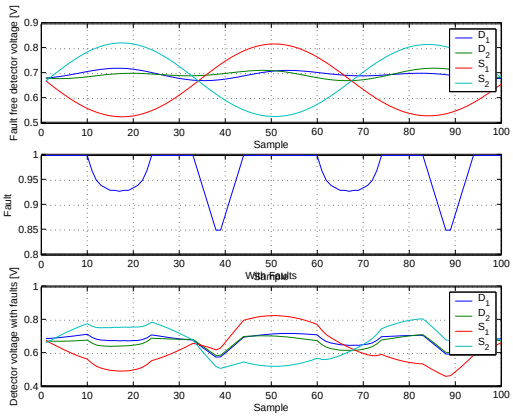

Figure 2. The four simulated detector signals without any faults, the fault, and the four simulated detector signals with faults.

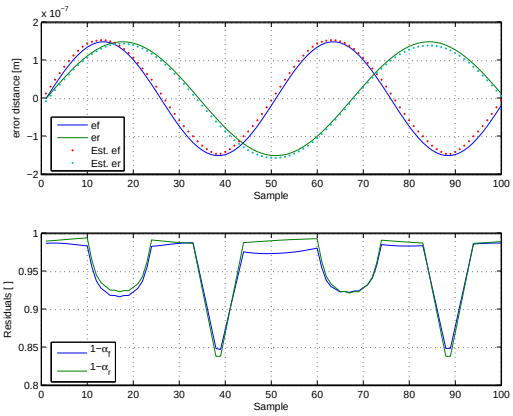

Figure 3. The upper plot compares the original focus and radial displacements with the ones computed by using the algebraic inverse map solver. The lower plot illustrates the computed residuals,representing the surface fault model. It can be seen that the error, introduced by the approximating polynomials, results in a deviation in the computed residuals.

due to approximation errors of the approximating polynomials. These errors can be neglected due to their relatively small sizes.

The computed residuals can be seen in the lower plot in Fig. 3. From this plot it can been seen that the residuals are computed well. However, some small deviations are present in the non-fault areas of the signal. These deviations are again due to errors in the approximating polynomials.

This means that except from errors in the approximating polynomials, this method gives an algebraic alternative to iterative method of computing the positions and fault parameters presented in (Odgaard *et al.* 2006) and (Odgaard 2004). Notice the iterative method for computing the inverse does use the same approximations, i.e. the iterative method cannot perform better than the algebraic method. It might even give a less accurate result, since the iterations might be stopped too early.

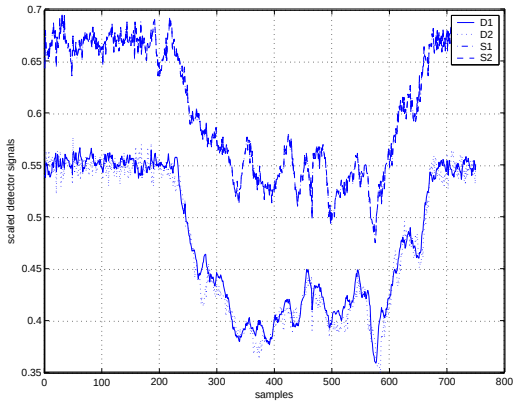

Figure 4. Measured detector signals $D_1[n], D_2[n], S_1[n]$ and $S_2[n]$ while passing the scratch.

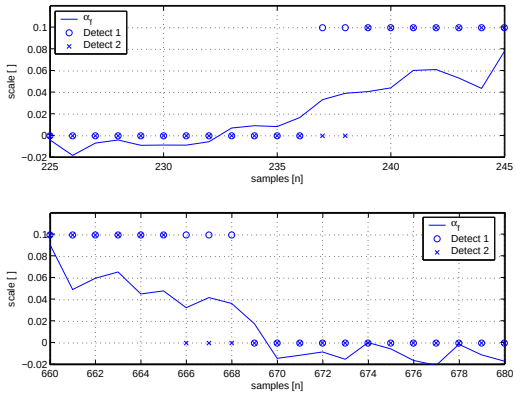

Figure 5. $\alpha_f[n]$ plotted together with detection signals based on both $\alpha_f[n]$ (Detect 1) and $S_f[n]$ (Detect 2). The upper plot shows the beginning detection of the scratch, and the lower plot shows the end detection

4.1 An example of the improved fault detection by the residual.

In subsection the improvements by using the computed residuals is compared with the standard used sums signals are illustrated. This is done by comparing the two different residual on a sampled scratch using a simple threshold. The original scratch can be seen in Fig. 6. The thresholds for the given signals are found such that they detect as much of the fault as possible and without making any false detections on the test data. These thresholds are found by a trial and error method. Fig. 4 which illustrates the scaled detector signals, from which it is easy to do a visual detection of the scratch. The real scratch is the part of the signals where the values are decreased. It lasts approximately from sample 230 to sample 670. The ideal fault detection algorithm will end up with these beginning and end detections of the scratch which, however, is a hard requirement to fulfill. Figs. 5 and 6 illustrates the beginning and end of the scratch seen in Fig. 4. From Figs. 5 and 6 it can be seen that $S_f[n]$, $S_r[n]$, $\alpha_r[n]$ and $\alpha_r[n]$ detect the fault well. The detections based on the

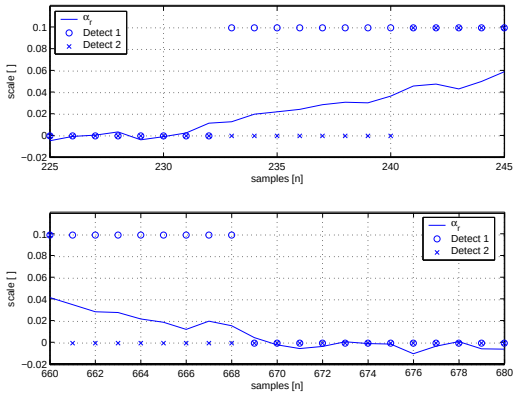

Figure 6. $\alpha_r[n]$ plotted together with detection signals based on both $\alpha_r[n]$ (Detect 1) and $S_r[n]$ (Detect 2). The upper plot shows the beginning detection of the scratch, and the lower plot shows the end detection.

four residuals are: the αs : $n = [233 - 668]$, the Ss : $n = [239 - 665]$. From these it can be seen that fault detection based on the new decoupled residuals $\alpha_f[n]$ and $\alpha_f[n]$ give a more clear detection than if the two other residuals were used, since the background noise level is lower. The new residuals have an improvement of 6 samples in the beginning and 3 samples in the end. This improvement seems less significant compared to the duration of the scratch, which is 441 samples. However, many practical experiments with fault tolerant control in CD-players have shown that an improvement of a few samples of the fault detection can result in a large controller performances improvement. One should also note that the new method for detection is very close to the fault localization by the visual inspection.

5. CONCLUSIONS

This paper presents an algebraic method for computing the decoupled residuals and positions of the OPU in a CD-Player. These residuals have previously been defined and computed using an iterative method in (Odgaard *et al.* 2006) and (Odgaard 2004). In this paper a new algebraic method is derived, and tested. This test shows that the algebraic method solves the problem finding the positions and residuals well, with a small error. This is due to errors in the approximating polynomials used to represent the model of the optical detectors in the CD-Player. Notice that the iterative method uses the same approximating polynomial splines, meaning that the algebraic method is as least as good as the iterative method.

6. ACKNOWLEDGMENT

The authors acknowledge the Danish Technical Research Council, for support to WAVES (Wavelets in Audio Visual Electronic Systems), grant no. 56-00-0143.

REFERENCES

Andersen, P., T. Pedersen, J. Stoustrup and E. Vidal (2001). Method for improved reading of digital data disc. International patent, no. WO 02/05271 A1.

Bierhoff, M.P.M. (1984). Apperatus for optimally scanning a disc-shaped record carrier. Patent US 4471477.

Bouwhuis, W., J. Braat, A. Huijser, J. Pasman, G. van Rosmalen and K. Schouhamer Immink (1985). *Principles of Optical Disc Systems*. Adam Hilger Ltd.

Chen, Jie and R. J. Patton (1999). *Robust model-based fault diagnosis for dynamic systems*. first ed.. Kluwer academic publishers.

Draijer, W., M. Steinbuch and O.H. Bosgra (1992). Adaptive control of the radial servo system of a compact disc player. *Automatica* **28**(3), 455–462.

Odgaard, Peter Fogh (2004). Feature Based Control of Compact Disc Players. PhD thesis. Department of Control Engineering, Aalborg University. ISBN:87-90664-19-1.

Odgaard, P.F., J. Stoustrup, P. Andersen and H.F. Mikkelsen (2003). Modelling of the optical detector system in a compact disc player. In: *Proceedings of the 2003 American Control Conference*. Denver, Colorado, USA. pp. 3101 – 3106.

Odgaard, P.F., J. Stoustrup, P. Andersen and H.F. Mikkelsen (2006). Detection of surface defects and servo signal restoration for a compact disc player. *IEEE Transactions on Control System Technology* **14**(2), 189–203.

Philips (1994). *Product specification: Digital servo processor DSIC2, TDA1301T*. Philips Semiconductors. Eindhoven, The Netherlands.

Steinbuch, M., G. Schoostra and O.H. Bosgra (1992). Robust control of a compact disc player. In: *Proceedings of the 31st IEEE Conference on Decision and Control*. Tucson, Arizona, USA. pp. 2596 – 2600.

Vidal Sánchez, Enrique (2003). Robust and Fault Tolerant control of CD-players. PhD thesis. Department of Control Engineering, Aalborg University. ISBN: 87-90664-15-9.